Lab on a Chip

Cite this: *Lab Chip*, 2012, **12**, 506

www.rsc.org/loc

FOCUS

Acoustofluidics 4: Piezoelectricity and application in the excitation of acoustic fields for ultrasonic particle manipulation

Jurg Dual* and Dirk Möller

DOI: 10.1039/c1lc20913b

Piezoelectric materials are widely used in the excitation of MHz frequency vibrations in devices for ultrasonic manipulation. An applied electrical voltage is transformed into mechanical stress, strain and displacement. Piezoelectric elements can be used in either a resonant or non-resonant manner. Depending on the desired motion the piezoelectric longitudinal, transverse or shear effects are exploited. Because of the coupling between electrical and mechanical quantities in the constitutive law the modelling of devices turns out to be quite complex. In this paper, the general equations that need to be used are delineated. For a one-dimensional actuator the underlying physics is described, including the consequences resulting for the characterization of devices. For a practical setup used in ultrasonic manipulation, finite element models are used to model the complete system, including piezoelectric excitation, solid motion and acoustic field. It is shown, how proper tailoring of transducer and electrodes allows selective excitation of desired modes.

Institute of Mechanical Systems, Department of Mechanical and Process Engineering, ETH Zentrum, CH-8092, Zurich, Switzerland

A Introduction

Exciting and detecting motion in solids and fluids by means of piezoelectric materials, in which an electric signal is converted into a mechanical motion and *vice versa*, has been used extensively also for ultrasonic particle manipulation. This method has several advantages.

- With the availability of programmable signal generators, waves of complex shape and frequency content can be produced with a high degree of repeatability, which opens the way to various signal processing techniques.

- By appropriate tailoring of the transducer set-up, different modes of waves and vibrations can be excited and measured selectively.

A necessary condition to make use of the above-mentioned advantages is the availability of materials with sufficiently high piezoelectric constants. This is the case in piezoelectric ceramics. While quartz has a piezoelectric charge constant of about 10^{-12} C N^{-1}, the same constant for Pz26, which is a modified lead zirconate titanate manufactured by Ferroperm Piezoceramics, amounts to 10^{-10} C N^{-1}.[1] The interaction between the piezoelectric transducer and the attached material will be described in the following. Basics regarding the theory can be found *e.g.* in ref. 2.

Piezoelectric materials have been used in ultrasonic particle manipulation from the very beginning. Red blood cells were segregated using planar ultrasound transducers.[3] Standing and travelling waves were used to manipulate cells for a number of applications.[4] The acoustic energy can be focussed by special non-planar transducers.[5,6] Modes can be selectively excited or two-dimensional patterns are formed by segmented transducers.[7,8] As an alternative, miniaturized transducers generate patterns of ultrasonic traps,[9] an approach that will be of increasing importance in view of improved methods to produce batch fabricated systems with piezoelectric elements. Shear transducers are suitable to excite bending vibrations in cover plates,[10] or piezoelectric LiNb crystals might be brought directly into contact with the fluid.[11] They are often used to generate surface acoustic waves by interdigitated electrodes.

A typical transducer as used in ultrasonics is shown in Fig. 1. It is brought in

Foreword

Piezoelectricity and piezoelectric transducers are pivotal for acoustophoretic devices. In this fourth paper of 23 in the tutorial series of Acoustofluidics in *Lab on a chip*, Jürg Dual and Dirk Möller describe the basic theory behind piezoelectricity and how the transducers can be used to excite mechanical vibrations into a material. A FEM model of an acoustic cavity including simulation of the fluidic and mechanical structure as well as the transducer is presented.

Andreas Lenshof – coordinator of the Acoustofluidics series

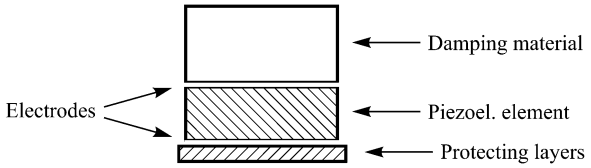

Fig. 1 Characteristic layout of a mounted piezoelectric element.

contact with the structure to be excited using a coupling agent or glue. Classical ultrasonic transducers work in a resonant mode, *i.e.* they have a defined frequency (resonance), at which they work best. Other transducers are used far below their resonance frequency and give a more broadband excitation.

When used in a continuous mode, one has to be careful not to heat up the transducer too much. This is particularly true for ceramic transducers, as they lose polarization when heated above their Curie temperature.

B Basic equations

Piezoelectric materials have an intrinsic polarization density $\boldsymbol{P}$. Depending on the direction of the applied electric field $\boldsymbol{E}$, which is controlled by the electrodes, extension/contraction (for $\boldsymbol{E}$ parallel to $\boldsymbol{P}$) or shear occurs (for $\boldsymbol{E}$ orthogonal to $\boldsymbol{P}$). In the following the linear theory of piezoelectric materials, which is suitable for a first approach to ultrasonic particle manipulation, is described. Therefore, the constitutive law is assumed to be linear. Nonlinear terms in the strain displacement relation are also neglected.

Constitutive relations for piezoelectric materials relate the four quantities (given together with their SI units)

E_i	Electric field	1st order tensor	N C^{-1}
D_i	Electric displacement	1st order tensor	C m^{-2}
γ_{ij}	Mechanical strain	2nd order tensor	—
σ_{ij}	Mechanical stress	2nd order tensor	N m^{-2}

by the material properties:

s_{Eijkl}	Mechanical compliance for constant electric field	4th order tensor	m^2 N^{-1}
d_{ijk}	Piezoelectric charge constant	3rd order tensor	C N^{-1} or m V^{-1}
$\varepsilon_\sigma = \varepsilon_{ij}$	Permittivity at constant mechanical stress	2nd order tensor	C^2 m^{-2} N^{-1}

The indicial notation is used, referring all quantities to an orthonormal base system with coordinates x_i, $i = 1, 2, 3$. Einstein's summation convention for repeated indices is invoked.

The electric displacement is defined as

$$D_i = \varepsilon_0 E_i + P_i, \tag{1}$$

where $\varepsilon_0 = 8.85 \times 10^{-12}$ C^2 N^{-1} m^{-2} is the vacuum permittivity. Eqn (1) expresses the fact that the electron cloud shifts with respect to the nucleus under the influence of an external electric field.

Constitutive equations for a piezoelectric material can then be given in the form

$$\begin{aligned} \gamma_\lambda &= s_{E\mu}\sigma_\mu + d_{k\lambda}E_k, \\ D_i &= d_{i\mu}\sigma_\mu + \varepsilon_{ik}E_k, \end{aligned} \tag{2}$$

where for simplicity Greek indices are introduced as in ref. 12. Greek indices take values from 1 to 6, and the correspondence between Greek matrix indices and pairs of Latin tensor indices is given by

ij	11	22	33	23, 32	13, 31	12, 21
λ	1	2	3	4	5	6

Jurg Dual

Jürg Dual has been Full Professor of Mechanics and Experimental Dynamics in the Center of Mechanics of the Institute of Mechanical Systems at the ETH in Zurich since October 1, 1998. Since 2008 he also has been President of the University Assembly of ETH in Zurich. Jürg Dual studied mechanical engineering at the ETH Zurich. He then spent two years on a Fulbright grant at the University of California in Berkeley, where he graduated with a MS and a MEng degree in mechanical engineering. He then received his Dr Sc. Techn. degree at the ETH Zurich. After one year as visiting assistant professor at Cornell University, Ithaca, NY, he returned to the ETH Zurich as assistant professor. He is a Fellow of the ASME, member of the SATW (Swiss Academy of Technical Sciences) and Honorary Member of the German Association for Materials Research and Testing. His research focuses on wave propagation and vibrations in solids as well as micro- and nanosystem technology.

Dirk Möller

Dirk Möller received the MSc degree in mechanical engineering from the Swiss Federal Institute of Technology, Zurich, in 2007, where he is currently pursuing the PhD degree at the Center of Mechanics. During his studies he focused on micro- and nanosystems. His main research area is ultrasonic manipulation within microfluidic devices.

It should be noted that piezoelectric ceramics have an axis of symmetry, which is parallel to the direction of poling. The material is transversely isotropic. It is customary to take the 3-direction as the axis of symmetry. The permittivity tensor is then diagonal with $\varepsilon_{11} = \varepsilon_{22}$. The tensor containing the charge constants is zero except for the elements d_{33}, $d_{31} = d_{32}$ and $d_{15} = d_{24}$.

Typical values for the material constants in extension and shear for Pz26 are summarized in Table 1.

Other materials have other material symmetries depending on their crystal structure.[2]

Particle manipulation is in most cases done using harmonic time signals. If the excitation voltage has the form $V = \mathrm{Re}(V_0 e^{i\omega t})$, also all other quantities will have the same time-dependence because of the linearity of the equations.

Therefore all quantities will have a time dependence of the form

$$A(\boldsymbol{r},t) = A(\boldsymbol{r})e^{i\omega t}. \tag{3}$$

In the following the exponential factor will be omitted, and it is understood that of all the quantities only the real part will have physical meaning.

The equation of mechanical equilibrium for the case of harmonic loading is then

$$\sigma_{ij,j} + \rho\omega^2 u_i = 0, \tag{4}$$

where $\boldsymbol{u}$, ρ and ω are the mechanical displacement, density and circular frequency, respectively, and $,_j$ is the derivative with respect to x_j.

The mechanical strain is defined as

$$\begin{aligned} \gamma_{ij} &= \frac{1}{2}\left(u_{i,j} + u_{j,i}\right), \\ 2\gamma_{ij} &= \left(1 + \delta_{ij}\right)\gamma_{\lambda}. \end{aligned} \tag{5}$$

Maxwell's first equation for dielectric materials is given as

$$D_{i,i} = 0. \tag{6}$$

The right hand side is zero, because there are no free charges in a dielectric material. Eqn (2)–(6) are the basic equations that need to be solved together with appropriate boundary conditions for the mechanical and electrical quantities. Normally the stress vector $s_i = \sigma_{ij}n_j$ and displacement u_i are assumed to be continuous across the interface of the transducer and the structure. If an electrical voltage V is applied across the electrodes a and b of the piezoelectric element, then

$$V = -\int_a^b \boldsymbol{E}\cdot \mathrm{d}\boldsymbol{r} \tag{7}$$

is the electrical boundary condition. The integral is a curve integral from a to b. The potential is spatially constant on electrodes, as they are conductive. On the other hand, for surfaces with no electrodes

$$\boldsymbol{D}\cdot\boldsymbol{n} = 0 \tag{8}$$

is the electrical boundary condition, where $\boldsymbol{n}$ is the unit normal.

For simplicity a uniaxial state will be assumed for both electrical and mechanical quantities in the analytical examples of Sections C and D. All coupling effects with other components of stress, strain, electric displacement and electric field will be neglected and also indices will be dropped for simplicity of writing. For more complicated situations, a finite element analysis is necessary (Section E).

Eqn (2) can be rewritten with σ and D as independent quantities:

$$\begin{aligned} \gamma &= s_{\mathrm{D}}\sigma + gD, \\ E &= -g\sigma + \frac{D}{\varepsilon}, \end{aligned} \tag{9}$$

where $g = d/\varepsilon$ is the piezoelectric voltage constant and $s_{\mathrm{D}} = s_{\mathrm{E}} - d^2/\varepsilon = s_{\mathrm{E}} - gd$ is the mechanical compliance for constant electric displacement.

In the uniaxial case one obtains from eqn (6)

$$D = D_0, \tag{10}$$

where D_0 is constant.

C Vibration of a free piezoelectric element excited by an applied electrical voltage

Referring to Fig. 2, the axial motion u of a slender transducer ($L \gg D$) with stress-free boundaries is considered. The stress state is uniaxial and the influence of lateral inertia is neglected in accordance with the theory for a slender bar.

Using eqn (4)–(10) one obtains the differential equation and boundary conditions

$$\begin{aligned} &u_{,11} + {k_{\mathrm{D}}}^2 u = 0, \\ &{k_{\mathrm{D}}}^2 = s_{\mathrm{D}}\rho\omega^2, \\ &u_{,1}(0) = gD_0, \\ &u_{,1}(L) = gD_0, \end{aligned} \tag{11}$$

which yield

$$u = \frac{gD_0}{k_{\mathrm{D}}}\left(\sin(k_{\mathrm{D}}x) + \frac{\cos(k_{\mathrm{D}}L) - 1}{\sin(k_{\mathrm{D}}L)}\cos(k_{\mathrm{D}}x)\right), \tag{12}$$

where k_{D} is the wavenumber and D_0 will be determined later. From eqn (5) and (9) the corresponding σ and E are computed:

$$\sigma = \frac{2gD_0}{s_{\mathrm{D}}}\left(\frac{\sin\left(\frac{1}{2}k_{\mathrm{D}}(L-x)\right)}{\cos(k_{\mathrm{D}}L/2)}\sin\left(\frac{k_{\mathrm{D}}x}{2}\right)\right),$$

$$E = \frac{D_0}{\varepsilon} - \frac{2g^2D_0}{s_{\mathrm{D}}}\left(\frac{\sin\left(\frac{1}{2}k_{\mathrm{D}}(L-x)\right)}{\cos(k_{\mathrm{D}}L/2)}\sin\left(\frac{k_{\mathrm{D}}x}{2}\right)\right). \tag{13}$$

The electric potential difference is given as

$$V = -\int_0^L E\,\mathrm{d}x = -\frac{D_0L}{\varepsilon} + \left(\frac{D_0g^2\left(2\tan\left(\frac{1}{2}k_{\mathrm{D}}L\right) - k_{\mathrm{D}}L\right)}{s_{\mathrm{D}}\,k_{\mathrm{D}}}\right). \tag{14}$$

Table 1 Material constants for Pz26 piezoelectric ceramic (ref. 1)[a]

	Units	Extension	Shear in plane orthogonal to $\boldsymbol{P}$
s_{E}	10^{-12} m^2 N^{-1}	$s_{\mathrm{E33}} = 19.6$	$s_{\mathrm{E55}} = 33.2$
s_{D}	10^{-12} m^2 N^{-1}	$s_{\mathrm{D33}} = 10.5$	$s_{\mathrm{D55}} = 23.1$
d	10^{-10} C N^{-1}	$d_{33} = 3.28$, $d_{31} = -1.28$	$d_{15} = 3.27$
ε	10^{-8} C^2 m^{-2} N^{-1}	$\varepsilon_{33} = 1.17$	$\varepsilon_{22} = \varepsilon_{11} = 1.06$
g	10^{-3} m^2 C^{-1}	$g_{33} = 28.0$, $g_{31} = -10.9$	$g_{15} = 38.9$
ρ	10^3 kg m^{-3}	$\rho = 7.7$	

[a] Mechanical compliances s_{E}, s_{D}, charge constant $d_{i\lambda}$, permittivity ε_{ij}, voltage constant $g_{i\lambda}$, density ρ.

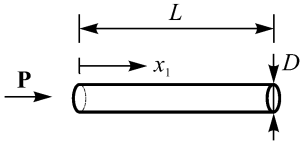

Fig. 2 Slender transducer ($L \gg D$) with stress-free boundaries and polarization density $\boldsymbol{P}$.

For a given applied voltage V_0, the resulting D_0 is inserted into eqn (12) to yield

$$u(0) = V_0 \frac{ds_D}{2s_E} \frac{\tan\left(\frac{1}{2}k_D L\right)}{\frac{1}{2}k_D L - k^2 \tan\left(\frac{1}{2}k_D L\right)}, \tag{15}$$

where $k^2 = gd/s_E$ is the electromechanical coupling coefficient, which describes how well electrical energy is converted into mechanical energy.

If in addition we impose $k_D L \ll 1$, eqn (12)–(15) can be simplified to yield for the quasistatic or "long wavelength" case:

$$\begin{aligned} D_0 &= -\frac{\varepsilon V}{L}\left(1 + O\left((k_D L)^2\right)\right), \\ u &= dV\left(\frac{1}{2} - \frac{x}{L}\right)\left(1 + O\left((k_D L)^2\right)\right), \\ \sigma &= 0 + O\left((k_D L)^2\right), \\ E &= -\frac{V}{L}\left(1 + O\left((k_D L)^2\right)\right), \end{aligned} \tag{16}$$

where $O(k_D L)$ denotes terms of order $k_D L$ and smaller. The transducer behaves electrically as a capacitor. Mechanically it contracts with constant strain, while the center of mass remains unmoved. The total length change ΔL is given by dV.

D Piezoelectric transducers used to excite mechanical vibrations in a structure

In the next step, a situation is considered, in which the element of Section C excites longitudinal motion in a circular rod (Fig. 3).

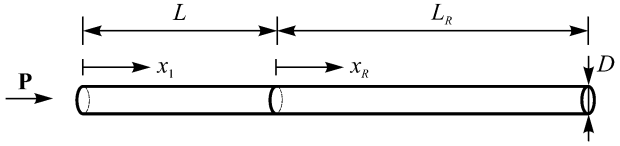

Fig. 3 Slender transducer ($L \gg D$) with length L and polarization density $\boldsymbol{P}$ coupled to a circular rod of equal diameter (L_R).

The transfer function between excitation voltage and the resulting motion is determined for the long wavelength case, *i.e.* the wavelength both in the transducer and in the rod is assumed to be much larger than the diameter of the rod and transducer. Again a uniaxial state of stress results for all elements involved.

To develop the equations the same procedure is used as before. The only differences are the boundary conditions, which now are

$$\begin{aligned} u_{,1}(0) &= gD_0, \\ u_{,1}(L) &= s_D\sigma_0 + gD_0. \end{aligned} \tag{17}$$

σ_0 is the stress between the transducer and the rod and can be expressed in terms of $u_0 = u(L)$ and the mechanical impedance Z_R of the rod:

$$\sigma_0 = i\omega Z_R u_0. \tag{18}$$

Dependent on the type of motion, the mechanical impedance is:

(a) for a wave propagation problem in an infinite rod

$$\begin{aligned} u &= u_0 e^{-ik_R x_R}, \\ k_R &= \frac{\omega}{c_R}, \\ c_R &= \sqrt{\frac{E_R}{\rho_R}}, \\ \sigma_0 &= -iE_R k_R u_0, \\ Z_R &= -\sqrt{E_R \rho_R}, \end{aligned} \tag{19}$$

where E_R and ρ_R are Young's modulus and density of the rod, respectively.

(b) for a vibration problem in a rod of length L_R and stress-free boundary at $x_R = L_R$

$$\begin{aligned} u &= u_0(\cos(k_R x_R) + \tan(k_R L_R)\sin(k_R x_R)), \\ \sigma_0 &= Ek_R u_0 \tan(k_R L_R), \\ Z_R &= -i\sqrt{E_R \rho_R}\tan(k_R L_R). \end{aligned} \tag{20}$$

One should note at this point that the mechanical impedance gets very small for the case of resonance ($k_R L_R = n\pi$), depending on the amount of damping.

For a weakly viscoelastic material in harmonic loading a complex modulus is introduced:[12]

$$E_R = E_0(1 + i\varphi),\ \varphi \ll 1 \tag{21}$$

$$\begin{aligned} k_R &= k_0(1 - i\varphi/2), \\ k_0 &= \frac{\omega}{c_0}, \\ c_0 &= \sqrt{\frac{E_0}{\rho}}, \end{aligned} \tag{22}$$

where φ is the loss angle of the rod material. In the case of resonance, where $\mathrm{Im}(Z_R) = 0$, and assuming $k_0 L_R \varphi \ll 1$

$$Z_R = -\sqrt{E_0 \rho_R}\ k_0 L_R\ \varphi/2. \tag{23}$$

From eqn (17) and (18) and using the same procedure as in Section C one obtains

$$\begin{aligned} D_0 &= \frac{V_0 k_D s_D}{g^2 \beta}, \\ \beta &= \sin(k_D L) + \alpha(\cos(k_D L) - 1) \\ &\quad - k_D L\left(1 + \frac{s_D}{dg}\right), \\ \alpha &= \frac{\cos(k_D L) - 1 - i(Z_R/Z_p)\sin(k_D L)}{\sin(k_D L) + i(Z_R/Z_p)\cos(k_D L)}, \end{aligned} \tag{24}$$

where Z_p is the characteristic mechanical impedance of the piezoelectric material.

$$Z_p = \sqrt{\frac{\rho}{s_D}}, \tag{25}$$

and

$$\begin{aligned} u &= \frac{V_0 s_D}{g\beta}(\sin(k_D x) + \alpha\cos(k_D x)), \\ \sigma &= \frac{V_0 k_D}{g\beta}(\cos(k_D x) - 1 - \alpha\sin(k_D x)), \\ E &= -\frac{V_0 k_D}{\beta} \\ &\quad \left(\cos(k_D x) - \alpha\sin(k_D x) - \left(1 + \frac{s_D}{dg}\right)\right), \\ G(\omega) &:= \frac{u(L)}{V_0} \end{aligned} \tag{26}$$

where G denotes the transfer function between the applied voltage and the displacement at the transducer interface. The electrical impedance Z as seen by the electrical network is computed from eqn (24) by

$$Z = \frac{V_0}{i\omega A D_0} = \frac{\beta g^2}{i\omega A k_D s_D}, \tag{27}$$

where A is the electrode area of the transducer. In the limit $k_D L \ll 1$, the above equations reduce to

$$
\begin{aligned}
D_0 &= -\frac{V_0\varepsilon}{L\psi},\\
u &= -\frac{V_0 d}{\psi}\left(\frac{x}{L}-\gamma\right),\\
\sigma &= \frac{V_0 d}{\psi}\rho\omega^2 L\left(\frac{x^2}{2L^2}-\gamma\frac{x}{L}\right),\\
E &= -\frac{V_0}{\psi L}\left(1-\gamma\frac{dg}{s_D}k_D^2 Lx\right),\\
\gamma &= \frac{(k_D L/2)+i(Z_R/Z_p)}{k_D L+i(Z_R/Z_p)},\\
\psi &= 1-\gamma\frac{dg}{s_D}\frac{(k_D L)^2}{2}.
\end{aligned}
\tag{28}
$$

If the transducer is used to excite waves, Z_R and Z_p have the same order of magnitude. Eqn (28) can be simplified and the transfer function $G(\omega)$ can be calculated:

$$
\begin{aligned}
\psi &= 1,\\
\gamma &= 1+\frac{i}{2}\frac{Z_p}{Z_R}k_D L-\frac{1}{2}\left(\frac{Z_p}{Z_R}k_D L\right)^2,
\end{aligned}
\tag{29}
$$

and

$$
G(\omega)=\frac{u(L)}{V_0}=\frac{d}{2}\frac{\omega\rho L}{\sqrt{E_R\rho_R}}\left(i+\frac{\omega\rho L}{\sqrt{E_R\rho_R}}\right). \tag{30}
$$

This expression for the transfer function can also be obtained directly by considering a rigid mass (transducer), the center of which is displaced by an amount $\Delta L/2 = dV_0/2$ relative to the interface with the rod. One obtains

$$
G(\omega)=\frac{d}{2}\frac{\omega}{\omega+i(Z_R/\rho L)}, \tag{31}
$$

and with eqn (19)

$$
G(\omega)=\frac{d}{2}\frac{\omega}{\omega+i\omega_C}, \tag{32}
$$

where

$$
\omega_C=\frac{\sqrt{E_R\rho_R}}{\rho L}.
$$

This result is equivalent to eqn (30) for $\omega \ll \omega_C$ and represents a high-pass behavior with ω_C as the cut-off frequency.

The magnitude of the transfer function for a typical configuration of transducer and rod is given in Fig. 4 for the exact solution according to eqn (24)–(26) and the rigid mass approximation of eqn (31). The magnitude is normalized to yield unity in the high frequency limit of eqn (31).

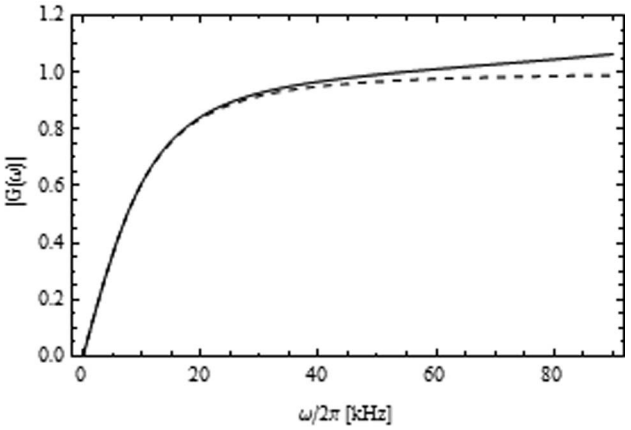

Fig. 4 Normalized magnitude of the transfer function for the excitation of waves in an infinite rod according to eqn (24)–(26) (solid) and eqn (31) (dashed) for the low frequency range. Transducer: Pz26, $L = 0.004$ m; rod: Lucite with $E_R = 5.29 \times 10^9$ N m^{-2}, and $\rho_R = 1.2 \times 10^3$ kg m^{-3}.

Up to a value of about twice the cut-off frequency of 12.7 kHz, eqn (31) is an excellent approximation. In this frequency range the transducer works off resonance resulting in low electromechanical coupling. For higher frequencies the effect of the transducer resonance is noticeable as an increase of the displacement amplitude.

A frequency range up to the first transducer resonance frequency is shown in Fig. 5. The amplitude gets very large for the resonance frequency of the transducer. These effects adversely affect wave propagation experiments, when it is desirable to have excitation which is constant over a wide frequency range. Digital filtering can be used to overcome the problem. On the other hand it is beneficial for cases where a high amplitude is sought at minimal applied voltage, which is often the case for ultrasonic manipulation devices.

The situation is different, if the transducer is used to excite resonance vibrations. In eqn (23) it is shown that the impedance of the rod Z_R in the vicinity of resonance is proportional to the loss angle φ and can be quite small. If we impose the condition for resonance

$$
\mathrm{Re}\left\{\frac{u(L)}{V_0}\right\}=0, \tag{33}
$$

assume $\varphi \ll 1$, $k_D L \ll 1$ and use the expression from eqn (20) for the impedance of the rod, a modified characteristic equation for the resonance is obtained:

$$
\varepsilon^* k_0 L_R + \tan(k_0 L_R) = 0, \tag{34}
$$

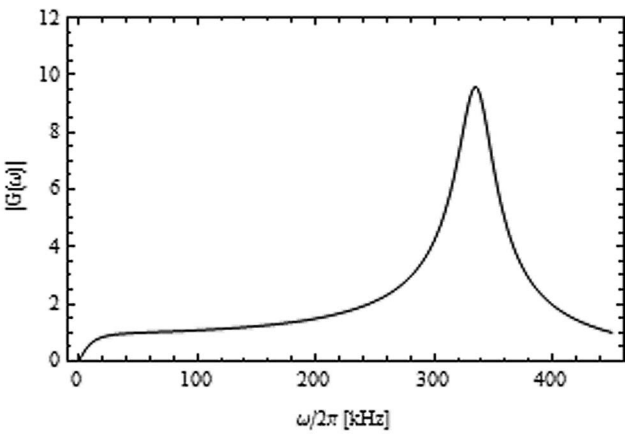

Fig. 5 Normalized (as in Fig. 4) magnitude of the transfer function for the excitation of waves in an infinite rod according to eqn (24)–(26) up to the first transducer resonance. Transducer: Pz26, $L = 0.004$ m; rod: Lucite with $E_R = 5.29 \times 10^9$ N m^{-2}, and $\rho_R = 1.2 \times 10^3$ kg m^{-3}.

with

$$\varepsilon^* = \frac{\text{mass of the transducer}}{\text{mass of the rod}}.$$

This corresponds to the characteristic equation for the resonance of a rod with an attached rigid mass. Using eqn (28) and (34), it can be shown that

$$\gamma = 1 - i\frac{\rho L}{\rho_R L_R \varphi} = 1 - i\frac{\varepsilon^*}{\varphi}, \qquad (35)$$

at resonance. For low damping φ, γ becomes very large and mechanical quantities in the transducer are completely dominated by a rigid mass type behavior: u is constant and the stress is linearly distributed.

Eqn (28) can only be simplified further for sufficiently high damping. Because dg/s_D is of the order 1, one is allowed to set

$$\psi = 1 \text{ for } \varphi \gg \varepsilon^*(k_D L)^2.$$

For this case the mechanical motion does not influence the electrical circuit, *i.e.* the coupling is low. Again the rigid mass approximation of eqn (31) yields the same result. On the other hand, if the damping is too small, very little energy pumped into the system will produce very large displacements, which in turn change the electric displacement. Then, no simplification of eqn (28) is possible.

The transfer function for a transducer which excites resonant vibrations is shown in Fig. 6. It is completely dominated by the resonances in the rod and the amount of damping present.

If we extend the frequency range and take a smaller rod length we obtain Fig. 7. At low frequencies, the peaks of the rod are visible, then they diminish in magnitude because of damping and increase again, because of the transducer resonance.

When characterizing devices for micromanipulation, very often the electrical impedance Z (eqn (27)) or admittance $1/Z$ for the transducer is plotted as shown in Fig. 8 and 9. It is seen that the low frequency peaks almost disappear, because of the low electromechanical coupling far away from the transducer resonance.

If we increase the damping ten times, all the system resonance peaks disappear and only the transducer resonance remains as seen in Fig. 10.

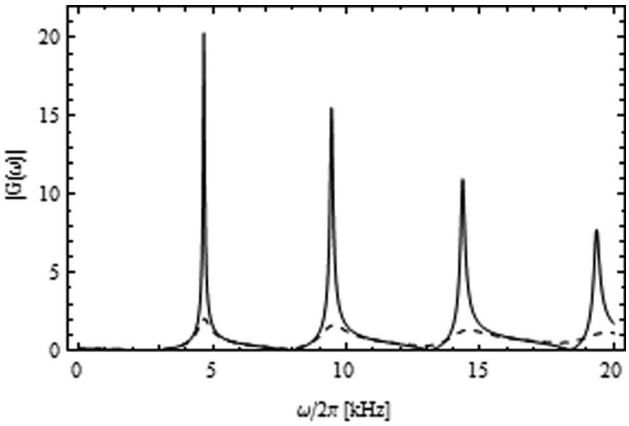

Fig. 6 Normalized (as in Fig. 4) magnitude of the transfer function according to eqn (24)–(26) for excitation of a resonant rod at low frequencies and two values of the damping φ: $\varphi = 0.01$ (solid) and $\varphi = 0.1$ (dashed). Transducer: Pz26, $L = 0.004$ m; rod: Lucite with $E_R = 5.29 \times 10^9$ N m^{-2}, $\rho_R = 1.2 \times 10^3$ kg m^{-3}, and $L_R = 0.2$ m.

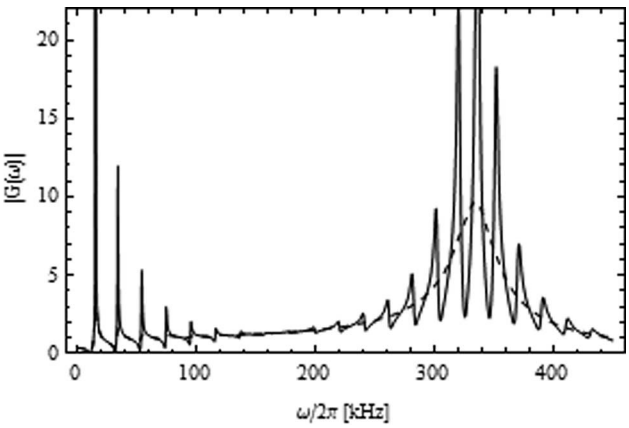

Fig. 7 Normalized (as in Fig. 4) magnitude of the transfer function according to eqn (24)–(26) for excitation of a resonant rod at higher frequencies and two values of the damping φ: $\varphi = 0.01$ (solid) and $\varphi = 0.1$ (dashed). Transducer: Pz26, $L = 0.004$ m; rod: Lucite with $E_R = 5.29 \times 10^9$ N m^{-2}, $\rho_R = 1.2 \times 10^3$ kg m^{-3}, and $L_R = 0.05$ m.

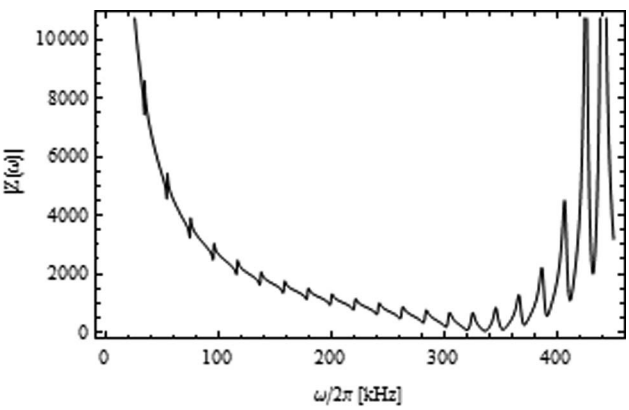

Fig. 8 Electrical impedance magnitude plot of the transducer according to eqn (24)–(27) for excitation of a resonant rod at higher frequencies and damping $\varphi = 0.01$. Transducer: Pz26, $L = 0.004$ m; rod: Lucite with $E_R = 5.29 \times 10^9$ N m^{-2}, $\rho_R = 1.2 \times 10^3$ kg m^{-3}, and $L_R = 0.05$ m.

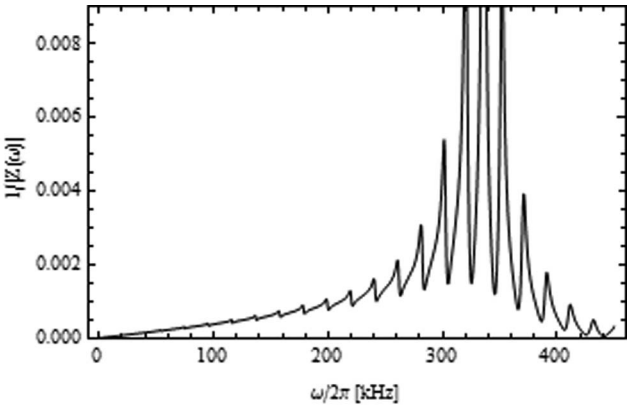

Fig. 9 Electrical admittance magnitude plot of the transducer according to eqn (24)–(27) for excitation of a resonant rod at higher frequencies and damping $\varphi = 0.01$. Transducer: Pz26, $L =$ 0.004 m; rod: Lucite with $E_R = 5.29 \times 10^9$ N m^{-2}, $\rho_R = 1.2 \times 10^3$ kg m^{-3}, and $L_R = 0.05$ m.

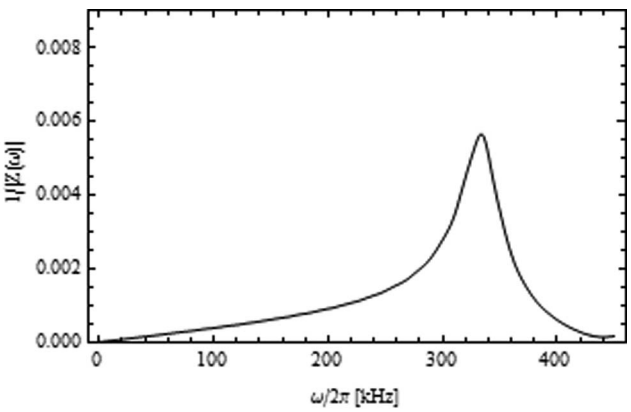

Fig. 10 Electrical admittance magnitude plot of the transducer according to eqn (24)–(27) for excitation of a resonant rod at higher frequencies and damping $\varphi = 0.1$. Transducer: Pz26, $L = 0.004$ m; rod: Lucite with $E_R = 5.29 \times 10^9$ N m^{-2}, $\rho_R = 1.2 \times 10^3$ kg m^{-3}, and $L_R = 0.05$ m.

This section has shown that even for a simple one-dimensional system there is a complex interplay between the transducer resonances and the system resonances that one wants to excite. Often in a device, these are tailored to coincide approximately in order to obtain maximum efficiency. However, as the transducer resonance itself depends on the structural impedance, this might not be an easy task. In addition, damping both within the system and within the piezoelectric element plays an important role.

E FEM model example of an ultrasonic cavity used for particle manipulation

A typical ultrasonic standing wave device consists of a fluidic domain, a surrounding mechanical structure and a piezoelectric transducer. For more complex models *e.g.* when going beyond 1D, a numerical simulation is a very strong tool. For the fluidic domain the acoustics problem needs to be solved. The mechanical parts can be described with a linear elastic material model and both the fluidics and the mechanical structure can be coupled with a fluid structure interaction. Such a model can be further extended with a piezoelectric material model.

While a numerical model is useful to find the resonance frequencies of a system it is also a strong tool to study and understand the response of the system. This can then be used to design or optimize the system further *e.g.* by performing parametric studies with different electrode layouts and different geometrical dimensions.

The resonating system model presented here is a typical microfluidic device for ultrasonic manipulation.[7] It consists of four domains as shown in Fig. 11. The base is a 5 mm × 0.5 mm piece of silicon with a 3 mm × 0.2 mm cavity filled with water. The cavity is sealed on top with a glass plate with the dimensions 5 mm × 0.5 mm. The transducer plate is attached to the silicon just below the fluidic cavity. It has the same width as the cavity with final dimensions of 3 mm × 0.5 mm. This piezoelectric element is driven in longitudinal mode with a strip of electrode.

The finite element method simulation presented here was performed in 2D and was done with COMSOL Multiphysics 4.2. For the four domains the following material properties have been used, where damping parameters are included as in eqn (21) with complex elastic constants:[13] silicon is an anisotropic material with a density of 2330 kg m^{-3} and components of the stiffness tensor of $c_{11} = 165.7$ GPa, $c_{12} = 63.9$ GPa and $c_{44} = 79.6$ GPa. Because in silicon the damping is very low, it is neglected here. The glass has a Young's modulus of $63(1 + i/400)$ GPa with a complex damping factor, a Poisson's ratio of $\nu = 0.2$ and a density of 2220 kg m^{-3}. Water has a density of 998 kg m^{-3} and a complex speed of sound of $1481(1 + i/2000)$ m s^{-1}. The piezoelectric material is Pz26 with a density given in Table 1 and a stiffness matrix with damping $\varphi = 1/180$ with the components $c_{E11} = c_{E22} = 168$ GPa, $c_{E33} = 123$ GPa, $c_{E44} = c_{E55} = 30.1$ GPa, $c_{E66} = 28.8$ GPa, $c_{E12} = c_{E21} = 110$ GPa and $c_{E13} = c_{E23} = c_{E31} = c_{E32} = 99.9$ GPa, a coupling matrix with the components $e_{15} = e_{24} = 9.86$ C m^{-2}, $e_{31} = e_{32} = -2.8$ C m^{-2}, and $e_{33} = 14.7$ C m^{-2} and a complex relative permittivity $(1 - i0.003)$ with the components $\varepsilon_{rS11} = \varepsilon_{rS22} = 828$ and $\varepsilon_{rS33} = 700$.

The fluid structure interaction is modeled with an inward acceleration for the acoustic domain and a boundary load defined as force per unit area for the mechanical structure. The outer mechanical boundaries are free. The electrodes of the piezoelectric element are indicated in Fig. 11. On the electrode shown in red a sinusoidal voltage of 20 V magnitude is applied, while the remaining electrodes shown in blue are set to ground. The other boundaries of the piezoelectric element are set with zero charge ($\boldsymbol{D}\cdot\boldsymbol{n} = 0$).

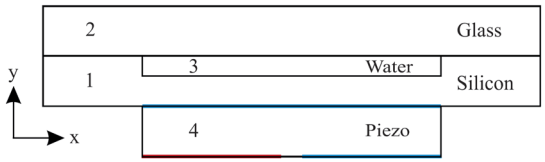

Fig. 11 Model of a microfluidic device for ultrasonic manipulation with electrode configuration (red = 20 V, blue = ground).

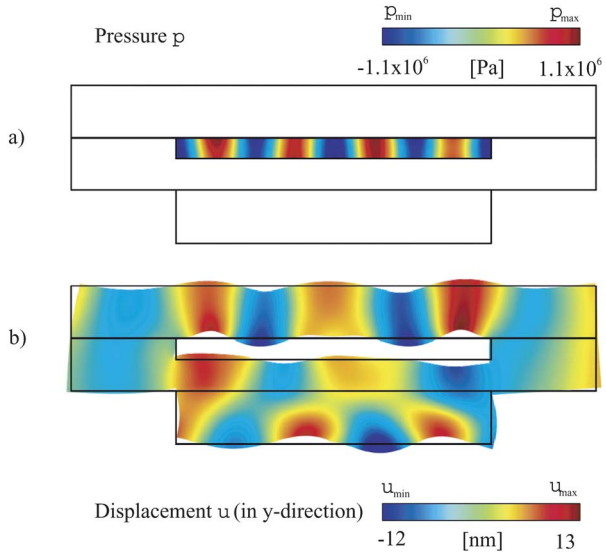

Fig. 12 (a) Pressure field in the fluid cavity at 1.9 MHz (b) displacement in the *y*-direction in color, total displacement outlined.

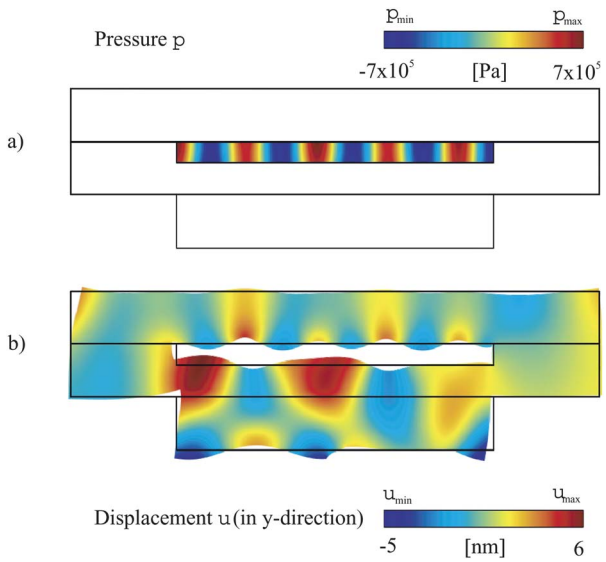

Fig. 13 (a) Pressure field in the fluid cavity at 2.15 MHz (b) displacement in the *y*-direction in color, total displacement outlined.

A frequency response analysis (frequency domain) was performed. The dependent variables are the pressure, the displacement field and the voltage. The stationary solver used is a direct MUMPS (MUltifrontal Massively Parallel sparse direct Solver) solver fully coupled. The system has been solved in a parametric study over a frequency range of 1.5–2.5 MHz with a step size of 500 Hz. Two characteristic modes within this range are presented here. Fig. 12 and 13 show a pressure resonant mode at 1.9 MHz and 2.15 MHz respectively. In figures (a) the pressure field is shown and in (b) the displacement in the *y*-direction is shown as a color graph where its outline shows the scaled up total displacement. Fig. 12 shows a symmetric pressure field with eight pressure nodal lines, whereas Fig. 13 shows an unsymmetrical pressure field with nine pressure nodal lines. Alternatively the symmetrical or antisymmetrical resonance could be suppressed by using an antisymmetrical or symmetrical electrode configuration, respectively. As an example, if the excited red electrode is arranged symmetrically with respect to the symmetry axis of the device in Fig. 11, only symmetrical modes are excited. Periodic arrangements of electrode patterns can be used to selectively excite corresponding wavenumbers.[11]

The quality of the pressure field is exemplary in the two cases presented here and can be reproduced for most of the higher and lower modes. While the pressure field at resonance is as expected the corresponding displacement field is more complex and hard to predict without a numerical simulation.

When experimenting with micromanipulation devices often temperature plays a crucial role. Because all the material properties are functions of temperature, the behavior of the device will change accordingly. Often the most important effect might be the temperature increase in glue layers, which will change the damping of the system and can drastically decrease the pressure amplitude in the cavity.

F Conclusions

The basic equations describing piezoelectric materials for their usage in ultrasonic manipulation devices have been described. A one dimensional system analysis of a transducer attached to a resonating bar has shown that a complex interplay exists between the resonances of the transducer and the structure, which is strongly influenced by the damping. This damping on the other hand depends on all the elements of the device, in particular also the glue layers which connect the transducer and the microfluidic chip. In electrical admittance

curves, the resonances will only show up, if there is strong electromechanical coupling. That is the system resonances must be reasonably close to the transducer resonance. The low coupling of the electrical circuit with the mechanical motion at frequencies far below the resonance frequencies of the piezoelectric transducer on the other hand allows broadband excitation at the expense of pressure amplitude in the device. For an actual device it has been shown that specific modes are selectively excited by special transducer setups, *e.g.*, using segmentation.

References

1 Ferroperm Piezoceramics A/S, http://www.ferroperm-piezo.com/.
2 V. M. Ristic, *Principles of Acoustic Devices*, Wiley, 1983.
3 N. V. Baker, Segregation and sedimentation of red blood cells in ultrasonic standing waves, *Nature*, 1972, **239**, 398.
4 W. T. Coakley, D. W. Bardsley, M. A. Grundy, F. Zamani and D. J. Clarke, *J. Chem. Technol. Biotechnol.*, 1989, **44**, 43.
5 H. M. Hertz, *J. Appl. Phys.*, 1995, **78**, 4875.
6 O. Manneberg, B. Vanherberghen, J. Svennebring, H. M. Hertz, B. Onfeld and M. Wiklund, *APL*, 2008, **93**, 063901.
7 A. Neild, S. Oberti and J. Dual, *Sens. Actuators, B*, 2007, **121**, 452.
8 A. Neild, S. Oberti and J. Dual, *JASA*, 2007, **121**, 778.
9 T. Lilliehorn, U. Simu, M. Nilsson, M. Almqvist, T. Stepinski, T. Laurell, J. Nilsson and S. Johansson, *Ultrasonics*, 2005, **43**, 293.
10 A. Haake and J. Dual, *Ultrasonics*, 2004, **42**, 75.
11 J. Friend and L. Y. Yeo, *Rev. Mod. Phys.*, 2011, **83**, 647.
12 J. Dual and T. Schwarz, *Lab Chip*, 2012, **12**, 244.
13 M. Gröschl, *Acustica*, 1998, **84**, 432–447.

